# SEMI-AUTOMATED DETECTION OF TERRAIN ACTIVITY IN THE SWISS ALPINE PERIGLACIAL ENVIRONMENT FROM DINSAR SCENES

**Barboux Chloé [(1)], Delaloye Reynald [(1)], Lambiel Christophe [(2)], Strozzi Tazio [(3)], Raetzo Hugo [(4)], Collet Claude [(1)]**

[(1)]*University of Fribourg, Geosciences department, Geography Unit (Switzerland), firstname.lastname@unifr.ch*
[(2)] *University of Lausanne, Institute of geography and sustainability (Switzerland), christophe.lambiel@unil.ch*
[(3)] *Gamma Remote Sensing (Switzerland), strozzi@gamma-rs.ch*
[(4)] *Federal Office for the Environment FOEN (Switzerland) hugo.raetzo@bafu.admin.ch*

## ABSTRACT

This paper proposes a semi-automated method to update inventory of moving slopes. First a Map of Terrain Activity (MTA) is created by partitioning an interferogram, using segmentation and classification processes, into 3 regions: stable areas, coherently moving parts and decorrelated areas (due to motion or not). Then, a Combined-Map of Terrain Activity (C-MTA) is computed describing the general behavior of the terrain at a specific time-lapse. Finally, C-MTA is used to determine the potential change in the activity rate of moving slopes. Tests are performed in a small area using large set of TSX DInSAR scenes from summers 2008 to 2012 in order to update past moving slope inventories produced from ERS DInSAR data.

## 1. INTRODUCTION

A large spectrum of mass wasting processes (e.g. landslides, rock glaciers, debris-covered glaciers) is actively changing the surface topography of alpine mountain slopes over time. The rate of motion is typically ranging from millimeter to several meters per year. The significant quantities of debris delivered downstream mass wasting slope may drastically change the debris flow activities in the subjacent gully and modify locally the exposure of settlements and transportation systems to damages on alluvial fans in the valley bottom. As a consequence, mass wasting processes may pose a significant threat to infrastructures as well as for lives of people living and moving in alpine terrain. Surveying systems are today mainly based on field observations, historically recorded events as well as experience and expert knowledge. Several sites are surveyed by geophysical investigations, some of them are actually surveyed by annual or seasonal DGPS (Differential Global Positioning System) campaigns, and even more by webcams and GPS installed on-site.

Regionally, the detection and characterization of slope motion above the tree line in the Swiss Alps has been performed using a large set of DInSAR (differential synthetic aperture radar interferometry) scenes dating back to the years 1991 to 1999 [1-4]. A large inventory of moving areas (hereafter called InSAR polygons) has been established in the periglacial belt. The exploitation of DInSAR data and the set-up of inventory have been carried out by visual interpretation on the basis of a large set of ERS interferograms comprising various time-lapses (from 1 day to 3 years) and polygons outline areas where DInSAR signals corresponding to a possible slope movement have been detected [2,5]. Current inventory is divided into signals of different magnitude order (>m/year, m/year, dm/year, cm/year) and contains signal patterns (~2000 in Western Swiss Alps) that are related to different mass wasting processes.

The main objective now is to – so far as possible – automatically update inventory by integrating the most recent data to detect potential change in activity rate of landforms. In order to obtain new information, a large set of TSX SAR data (2008-2012) is used, analyzed and interpreted. The process presented here uses segmentation and classification methodologies applied on interferometric coherence and phase images to detect the activity of the terrain within DInSAR scenes. Then, the resulting map of terrain activity is used to update inventory of InSAR polygons.

## 2. METHODOLOGY

### 2.1. Terrain activity analysis

The main goal of this analysis is to partition an interferogram into 3 regions: stable areas, coherently moving parts and decorrelated areas (due to motion or not). Decorrelated areas are first detected using noise filtering applied on interferometric coherence image. Then, a region growing algorithm applied on interferometric phase image is used to determine if the remaining pixels are moving or stable. Finally, the process is applied to a set of interferograms having same time-lapse to determine a Combined Map of Terrain Activity (Fig. 1).
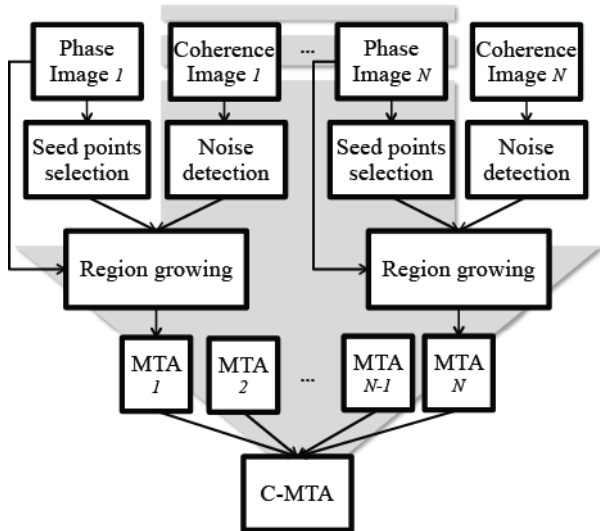
*Figure 1: From interferometric phase and coherence images to Combined-Map of Terrain Activity (C-MTA). Process applied to a selected set of N interferograms having the same time-lapse.*

### a) Noise filtering

The method consists in detecting noisy areas in the interferogram by thresholding the interferometric coherence. This process allows classifying decorrelated areas.

### b) Seed points selection

The first step in region growing is to select seed points. From the interferogram, the activity of pixel evenly spaced on a grid is visually determined according to the 3 categories. Stable points are then selected as initial seed points for the region growing algorithm.

### c) Region growing

Finally, a standard region growing algorithm is applied on the interferometric phase to segment the reminding areas into stable or moving areas [6]. This approach examines neighboring pixels from initial stable seed points and determines whether or not they should be added to the stable region. Regions are grown from stable seed points to adjacent 4-connected neighborhood depending on a region membership criterion:

$$\Delta\phi > \frac{\lambda}{2} \cdot RG_c \qquad (1)$$

With $\Delta\phi$ the variation of interferometric phase between two neighboring pixels
and $RG_c$ the region membership criterion

### d) Map of Terrain Activity (MTA)

The resulting map is thus classified into 3 classes: stable areas, coherent moving areas and noisy areas (due to motion or not).

### d) Combined-Map of Terrain Activity (C-MTA)

By applying this process to several interferograms having the same time-lapse and by combining the classification results; the general behavior of the terrain is obtained at a specific time-lapse. Pixels are thus classified into each of the 3 categories the most represented by the selected interferograms. An extra class is added indicating when the algorithm is not able to clearly classify the pixel (class NaN). An additional map has been produced to give an index of reliability concerning the classification of each pixel point. This one is performed on the idea that the more the number of images used for the classification and the number of images classifying the pixel in one specific class are high, the more the classification is reliable (Fig. 2).
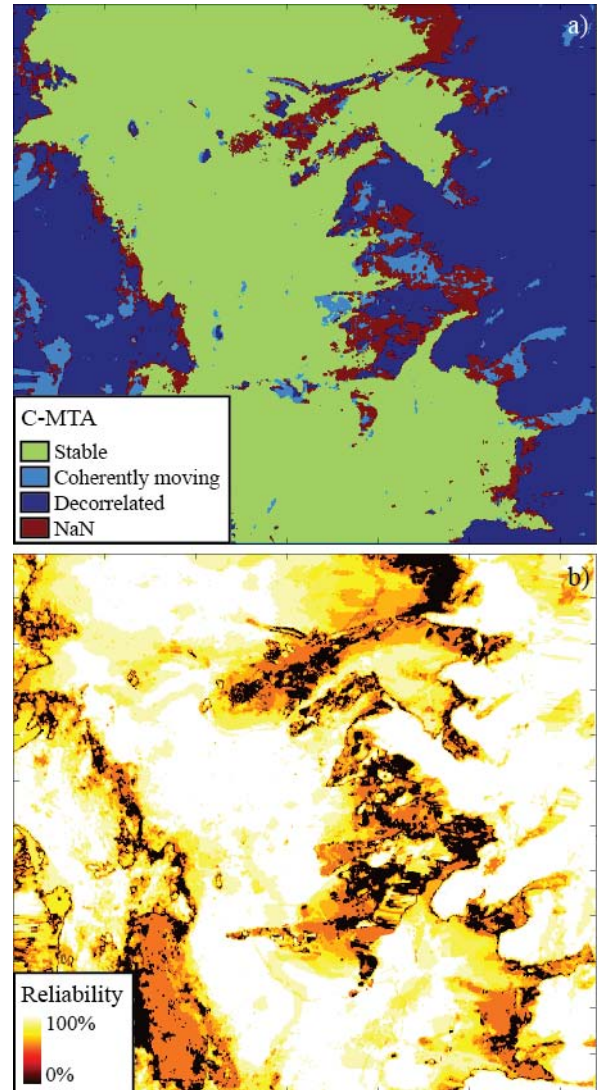


*Figure 2: a) Resulting C-MTA and respective b) Reliability index for the studied area with a time-lapse of 11 days. Seed points evenly spaced on a grid of 500m, $RG_c=1/8$.*

### 2.2. InSAR Polygons inventories update

#### a) Variation of terrain activities analysis

In order to detect the potential change in the activity rate of InSAR polygons from past inventories, each of them is automatically compared with the C-MTA to see the surface proportion in each class of terrain activity according to time-lapse (fig. 3).
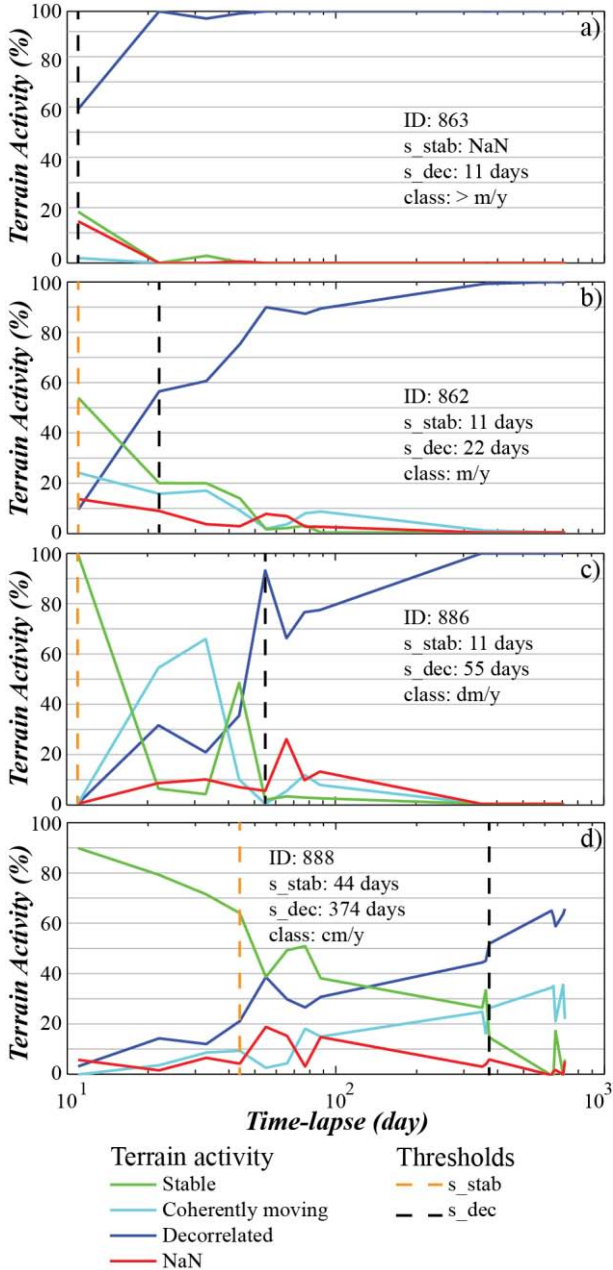


*Figure 3: Terrain activities of selected InSAR polygons moving at the velocity rate of a) >m/y, b) m/y, c) dm/y and d) cm/y*

#### b) Magnitude order of the displacement rate update

Then, two thresholds are detected: 1) *s_stab* corresponding to the time-lapse where the proportion of stable pixels decreases below 50% and 2) *s_dec* corresponding to the time-lapse where the proportion of noisy pixels is higher than 50%. Time-lapses in between these two thresholds represent the period where coherent movement can be observed (fig. 3). The displacement rate is then evaluated into 4 categories, namely: cm/y, dm/y, m/y and >m/y.

Finally, this value is compared with previous magnitude order for further updating.

### 3. RESULTS

The method was tested in a small studied area of 37 km$^2$ using 140 pairs of TSX data scenes from summers 2008 to 2012 with different time-lapses (Tab. 1).

| Time-lapse | Number of pairs |
|:---:|:---:|
| 11 days | 11 |
| 22 days | 10 |
| 33 days | 10 |
| 44 days | 10 |
| 55 days | 10 |
| 66 days | 9 |
| 77 days | 12 |
| 88 days | 11 |
| 352d | 12 |
| 363d | 7 |
| 374d | 8 |
| 638d | 6 |
| 649d | 5 |
| 660d | 5 |
| 704d | 6 |
| 715d | 8 |
| **Total** | **140** |

*Table 1. Number of selected interferograms*

### 3.1. C-MTA performance using qualitative observations

The number of seed points and the value of the region membership criterion $RG_c$ can influence the resulting C-MTA. To test these parameters, a selection of seed points were visually detected on a grid evenly spaced on the studied area of 1000, 500, 250 and 100 meters. $RG_c$ was fixed to 1/16, 1/8 and 1/4. Results on C-MTA show that smaller $RG_c$ is, more quickly the region growing algorithm stops, and smaller the resulting stable area is. The number of seed points does not shows big differences in the resulting C-MTA, though some distinctive areas are not grown when they are not described by a seed point. Finally, the algorithm classifies with difficulty outlines in between two neighboring categories with smaller dataset of seed points resulting in a kind of border effect where pixels are uncategorized (class NaN).

### 3.2. InSAR Polygons semi-automated update performance

To avoid influence of semi-automated velocity classification, each polygon was previously checked manually to verify the current velocity and the potential upgrade concerning outline if need be. As the aim of this semi-automated update is to detect which polygon has a change in velocity; a Confusion Matrix *CM* related to the change in velocity detection is computed. *CM* counts the number of polygons assigned to a change in the activity rate by the algorithm against reference visually interpreted. The diagonal values of *CM* represent the correctly classified samples. $CM_{pct}$ is the relative confusion matrix.

$$AE = 100 - mean(diag(CM_{pct})) \qquad (2)$$

$$CR = \frac{100 \cdot \sum diag(CM)}{\sum sample} \qquad (3)$$

With *AE* the global Average Error and *CR* the Correct Rate of classification.

| | AE (%) | | classified as | |
|---|---|---|---|---|
| | **27.38** | | change | no change |
| **%** | Change | *100* | 78.57 | 21.43 |
| | No change | *100* | 33.33 | 66.67 |
| | **Sensitivity** | 78.57 | **Specificity** | 66.67 |
| | CR (%) | | classified as | |
| | **70.45** | | change | no change |
| **Samples** | Change | *14* | 11 | 3 |
| | No change | *30* | 10 | 20 |
| | **Sensitivity** | 0.79 | **Specificity** | 0.67 |

*Table 2. Comparative Classification Performance (Confusion matrices) of automatic and manual change in velocity detection on selected InSAR polygons*

The number of seed points and the value of the region membership criterion $RG_c$ do not at all influence the resulting update of InSAR polygons which are always classified in the same categories of velocity.

### 3.3. Final manual upgrade

Fig. 4a shows results of the semi-automated change in velocity detection using the presented methodology. Fig. 4b shows the manual upgrade of the studied area performed before processing the semi-automated velocity classification (without a priori knowledges). A lot of InSAR polygons have been spared into different objects. And numerous new moving objects are found.
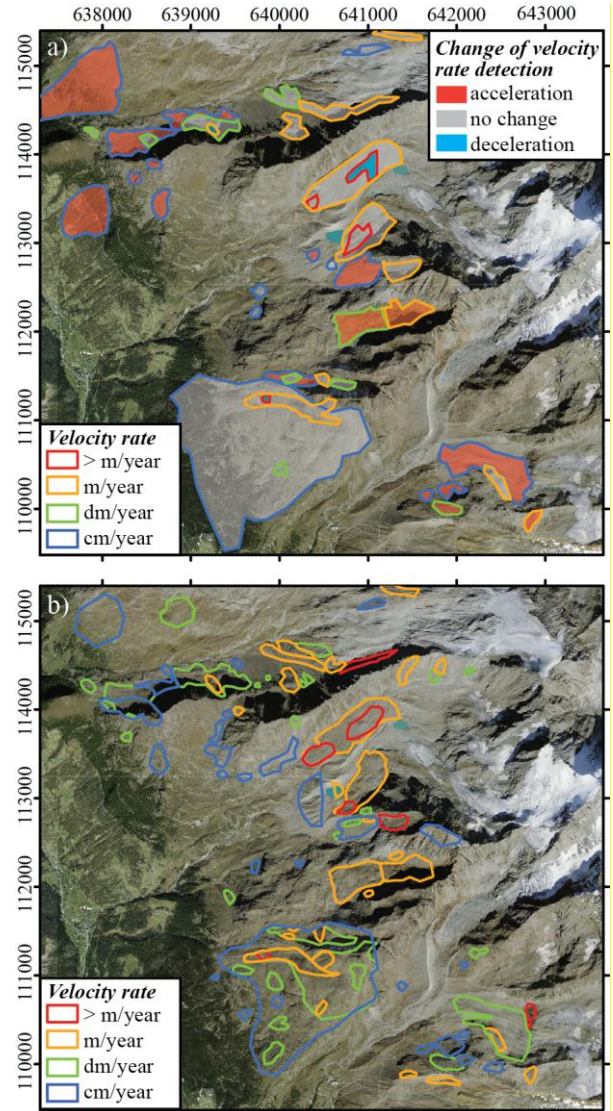


*Figure 4. InSAR polygons of the studied area. a) Past InSAR polygons inventory and result of semi-automated change in velocity rate detection. b)Manual upgrade of InSAR polygons.*

## 4. DISCUSSION

Region growing is a simple method which can only provide good segmentation results for images with clear edges. To grow a distinctive stable area, at least one seed point is needed in this region. In our case, the choice of visually determining a dataset of seed points evenly spaced on a grid seems to solve the problem, especially with high resolution. Nevertheless, determining a large set of seed points is extremely time consuming, especially when it is done manually.

Concerning InSAR polygons update, we observe acceptable performances using semi-automated methods (Average Error 27.38%, Correct Classification Rate 70.45%). Moreover the sensitivity – ability to identify change in the velocity rate – is high, 78.57% of the

changing polygons are correctly identified by the algorithm.

Only 3 changing polygons were incorrectly identified as not changing. Two of them concerns rock glaciers whose current velocity was visually attributed with difficulty. The last one concerns a moraine whose activity is not visible any more. Due to noise effect, the region is decorrelated using 2 years' time-lapses. Thus the polygon is incorrectly classified as moving with the same deformation rate of cm/y.

False detection is mainly due to external factors as vegetation, snow or atmosphere (where the signal is noisy), due to border effect in neighboring areas, due to large seasonal variation of the velocity, as well as due to a change of the outline of the landform.

The new high-resolution of X-Band TSX permits a better information about the landform outline and the landform displacement rate. Especially, its short X-Band wavelength combined with short repeated cycle allows parsing the structure of four categories of velocity rate into more precise subcategories. In other words, new sensors permit to update inventory (in term of current deformation rate quantification) but also to upgrade them (in term of identification of the landform outline and finer quantification of landform displacement rate). However, when performing such inventories, the compatibility between different sensors has to be considered in order to allow future updates. Thus the old classification system of velocity rate is conserved.

The presented method allows easily identifying InSAR polygons having change in velocity and is powerful to update past inventory. However, to perform the upgrade of the inventory, each of these changing InSAR polygons has to be manually checked in order to verify if the change is really due to change in velocity rate and/or if the outline has to be modified. At regional scale, first observations show that a large number of polygons are changing. Some landforms show current reactivation while others are slowing down. A lot of InSAR polygons have to be divided into different objects and numerous new moving objects are visually found due to the better definition of TSX data. Finally, the major conclusion from this study is that it is probably not advisable to automatically detect polygons having change in velocity from the new TSX data if they were previously derived from another sensor, as here, derived from ERS data.

## 5. CONCLUSION

The process presented here uses segmentation and classification methodologies applied on interferometric coherence and phase images to detect the activity of the terrain within DInSAR scenes. Then, the resulting Combined Maps of Terrain Activity (C-MTAs) are used to automatically update inventory of InSAR polygons.

The use of these maps was tested in a small studied area using large set of TSX DInSAR scenes from summers 2008 to 2012 in order to update past moving slope inventories. The model to create C-MTA is simple but robust and the classification of the terrain activity is much more reliable by using several DInSAR pairs. Moreover, the method to detect change in velocity of InSAR polygons works reliably. False change detection is mainly due to external factors as vegetation, snow or atmosphere (where the signal is noisy), due to border effect in layover and shadow areas, as well as due to a change of the outline of the landform.

The method is powerful to update inventory. However, to upgrade them, each of the detected changing InSAR polygons has to be manually checked. And a lot of new polygons are not detected.

The idea now is to explore the ability to use C-MTAs to detect new moving areas, as well as to assist in the development of accurate inventory as a useful tool for visual interpretation of DInSAR data.

## 7. REFERENCES

1. Delaloye R, Lambiel C, Lugon R, Raetzo H, Strozzi T. 2007. ERS InSAR for Detecting Slope Movement in a Periglacial Mountain Environment (Western Valais Alps, Switzerland). *Proceeding of HMRSC-IX, Grazer Schriften der Geographie und Raumforschung* **43** : 113–120.

2. Delaloye R, Lambiel C, Lugon R, Raetzo H, Strozzi T. 2007. Typical ERS InSAR signature of slope movement in a periglacial mountain environment (Swiss Alps). *Proceeding of ENVISAT Symposium 2007* (ESA SP-636, July 2007).

3. Delaloye R, Strozzi T, Lambiel C, Perruchoud E, Raetzo H. 2008. Landslide-like development of rockglaciers detected with ERS 1-2 SAR interferometry. *Processing of FRINGE 2007 Workshop* (ESA SP-649, February 2008).

4. Delaloye R, Strozzi T, Lambiel C, Barboux C, Mari S. 2010. The contribution of InSAR data to the early detection of hazardous active rock glaciers in mountain areas. *Proceedings ESA Living Planet Symposium 2010*, (ESA SP-686, December 2010).

5. Lambiel C, Delaloye R, Strozzi T, Lugon R, Raetzo H. 2008. ERS InSAR for assessing rock glacier activity. *9th Int. Conference on Permafrost 2008* : 1019–1025.

6. Caloz, R. et Collet, C. (2001) Précis de télédétection, Volume 3 - Traitement numérique d'images de télédétection. Presses de l'Université du Québec 386 p.